Pergamon

www.elsevier.com/locate/jaerosci

PII: S0021-8502(99)00020-8

J. Aerosol Sci. Vol. 30, No. 9, pp. 1191–1199, 1999

Printed in Great Britain
0021-8502/99/$ - see front matter

AEROSOL PARTICLE SIZE GROWTH BY SIMULTANEOUS COAGULATION AND CONDENSATION WITH DIFFUSION LOSSES IN LAMINAR FLOW TUBES

M. Alonso,*† F. J. Alguacil,* M. I. Martin,* Y. Kousaka‡ and T. Nomura‡

* National Center of Metallurgical Research, Avenida Gregorio del Amo, 8 28040 Madrid, Spain
‡ Department of Chemical Engineering, Osaka Prefecture University, 1-1 Gakuencho, 599-8531 Sakai, Japan

(*First received* 10 *June* 1998; *and in final form* 17 *December* 1998)

Abstract—The growth process of evaporation–condensation aerosol particles by simultaneous Brownian coagulation and condensation in a laminar flow tube downstream the particle generation unit has been studied. Size growth has been modeled assuming that vapor concentration in the tube just after the generator is already very low (negligible self-nucleation). The model, which also accounts for particle diffusion losses, permits an easy estimation of the coagulation and condensation rates. The effect of the generator cooling temperature on the relative importance of coagulation and condensation in the after-generation particle growth process has been examined. Experiments have shown that aerosols generated by traditional evaporation–condensation methods still grow by condensation much after they have left the generator. © 1999 Elsevier Science Ltd. All rights reserved

INTRODUCTION

Evaporation–condensation is a technique widely used for the generation of aerosols, because it allows the precise control of particle size distribution and concentration over a relatively wide range. The method consists basically of two steps: formation of a vapor phase by heating a solid or liquid sample, and subsequent cooling to condense the vapor molecules. The nucleated particles then grow by two simultaneous mechanisms: condensation of the remaining vapor molecules onto their surface, and Brownian coagulation among the particles themselves.

In experimental research, the generation of detectable amounts of nanometer-sized particles, for which diffusion loss is very high, requires minimization of the aerosol residence time in the system. This can be accomplished by increasing the aerosol flow rate and/or decreasing the volume of the system elements (heating and cooling sections, tubing, connections). There are limitations, however, because insufficient residence time may give rise to relatively large amount of vapor molecules still present far beyond the evaporation–condensation generator. Thus particles may still be growing by vapor condensation after they have left the generator. The purpose of the present investigation is to evaluate the magnitude of this after-generation condensational growth effect.

The aerosol evolution (size distribution, number concentration) in the process can be rigorously described by the general dynamic equation (GDE) (Friedlander, 1977). A number of authors (among others, Pesthy *et al*., 1983; Warren and Seinfeld, 1985; Seigneur *et al*., 1986; Pratsinis, 1988; Phanse and Pratsinis, 1989; Lazaridis and Koutrakis, 1997; Katoshevski and Seinfeld, 1997) have numerically solved the GDE considering all or only a part of the possible mechanisms affecting the aerosol dynamics (nucleation, condensation, evaporation, coagulation, diffusion losses, etc.).

In many instances, some of the aerosol mechanisms cited above are negligible, and this gives rise to more tractable approaches. Thus, aerosol particle growth by condensation in laminar flow tubes has been treated by Davis and Liao (1975), Zhang and Liu (1990) and Wilck and Stratmann (1997), but none of these authors considered coagulation. Wu and

† Author to whom correspondence should be addressed.

Biswas (1998) proposed the estimation of the relative importance of condensation and coagulation on particle size growth in terms of characteristic times. However, they considered systems in which only one of these two mechanisms is present. A more realistic treatment, considering simultaneous coagulation and condensation but not diffusion losses, has been developed by Jain *et al.* (1997), who studied a system of a relatively low aerosol concentration in which particle size growth is dominated by condensation.

In this paper we attempt to describe the size growth of nanometer aerosols in laminar flow tubes by simultaneous coagulation and condensation, taking also into account diffusion losses to the walls, but neglecting new particle formation by self-nucleation. The proposed model is then used to evaluate the coagulation and condensation rates in order to assess the relative importance of both mechanisms in the downstream growth of aerosol particles generated by a conventional evaporation-condensation method.

SIMPLIFIED MODEL

The system to be modeled consists of aerosol particles and vapor "molecules" of the same material as the particles, flowing laminarly through a test tube. Aerosol particles grow by two simultaneous mechanisms: (a) coagulation among particles, and (b) condensation of vapor molecules onto the particles. At the same time, aerosol particles are lost by diffusion to the tube wall. For simplicity, we will assume a monodisperse aerosol throughout the process (or, equivalently, only the mean particle size will be considered). It is also assumed that, since at the tube inlet (time $t = 0$) particle concentration is quite high and vapor concentration relatively low, the vapor molecules condense preferentially onto the surface of already formed particles, that is, the formation of new particles in the tube by homogeneous nucleation is assumed to be comparatively negligible.

The total number concentration N of aerosol particles decreases with time due to Brownian coagulation and diffusion losses to the wall. Regarding coagulation, we will use a size-independent coagulation rate constant K. The mean particle size increases by coagulation and condensation and, therefore, the coagulation rate constant K is actually a function of time. In the kinetic regime, the coagulation rate constant for collisions between equal-sized particles increases with the square root of the particle diameter. In the experiments to be discussed below the maximum ratio of final to initial mean particle diameter was about 1.4; this means that at the end of the process the coagulation rate constant was, at most, 1.18 times larger than at the beginning (smaller than 1.18 for experiments with shorter aerosol residence time). Thus the assumption of a time-independent coagulation rate constant is justified.

On its part, particle diffusion losses to the tube wall can be evaluated by means of the Gormley–Kennedy equation (Gormley and Kennedy, 1949). This equation, valid for laminar flow, expresses particle penetration P as a function of the parameter $\beta = Dt/R^2$ (D = diffusion coefficient; t = time; R = tube radius):

$$P = 0.8191\mathrm{e}^{-3.657\beta} + 0.0975\mathrm{e}^{-22.3\beta} + 0.0325\mathrm{e}^{-57\beta} \quad \text{for } \beta \geqslant 0.0312, \tag{1a}$$

$$P = 1 - 2.56\beta^{2/3} + 1.2\beta + 0.177\beta^{4/3} \quad \text{for } \beta < 0.0312. \tag{1b}$$

It has recently been shown that these equations are accurate for particle diameter down to about 2 nm (Alonso *et al.*, 1997a). Penetration at time t can be expressed as $P(t) = N(t)/N_0$, where $N(t)$ is the aerosol particle number concentration at time t, and N_0 is the number concentration at $t = 0$ (tube inlet). The variation of the particle number concentration with time due to diffusion losses should then be evaluated as $(\mathrm{d}N/\mathrm{d}t)_{\mathrm{diff}} = N_0(\mathrm{d}P/\mathrm{d}t)$, where $\mathrm{d}P/\mathrm{d}t$ should be found from equation (1). Instead of doing this, we will use a simplified approach, consisting in assuming that diffusion loss is simply proportional to the particle number concentration, $(\mathrm{d}N/\mathrm{d}t)_{\mathrm{diff}} = -\delta N$, where δ is the diffusion loss rate constant. According to this approximate model, penetration is given as $P = \mathrm{e}^{-\delta t}$.

With all the above considerations, the time variation of the particle number concentration can be expressed as

$$\frac{dN}{dt} = -\frac{1}{2}KN^2 - \delta N. \tag{2}$$

Integration of (2) with initial condition $N = N_0$ at time $t = 0$ yields

$$N = \frac{N_0 e^{-\delta t}}{1 + (KN_0/2\delta)(1 - e^{-\delta t})}. \tag{3}$$

Substituting P for $e^{-\delta t}$, equation (3) can be rewritten as

$$\frac{PN_0}{N} - 1 = R_{coag}\frac{(1-P)}{-\ln P}t, \tag{4}$$

where

$$R_{coag} \equiv \tfrac{1}{2}KN_0 \tag{5}$$

is the *coagulation rate* (dimensions of time^{-1}.) The coagulation rate R_{coag} can be determined from experiments using equation (4).

Consider now a system in which condensation does not occur, i.e. a system where particle size growth is only due to Brownian coagulation. In this special case, the total particle volume balance is

$$PN_0v_0 = Nv \quad \text{(no condensation)}, \tag{6}$$

where v is the mean particle volume diameter, and the subscript 0 refers to time $t = 0$. Combining equations (3) and (6) one arrives at

$$v = v_0\left[1 + \frac{R_{coag}}{\delta}(1 - e^{-\delta t})\right] \quad \text{(no condensation)}. \tag{7}$$

Thus, in a system where coagulation dominates, the mean particle volume increase rate is given by

$$\left(\frac{dv}{dt}\right)_{coag} = R_{coag}v_0 e^{-\delta t} = R_{coag}v_0 P. \tag{8}$$

Since penetration P decreases with time, the rate of particle volume increase by coagulation also decreases with time. If diffusion losses had been neglected, the particle volume would increase (by coagulation) linearly with time at a constant rate $R_{coag}v_0$.

According to equation (6), if there is no condensational growth the total particle volume should decrease with time, i.e. $Nv < N_0v_0$, because $P < 1$. On the contrary, the experimental results (to be discussed later) show that the total particle volume increases with time. This argument will be further developed to demonstrate that vapor condensation does indeed take place beyond the aerosol generator.

We now turn our attention to the other growth mechanism present in the system. In the free molecular regime, the particle volume increase with time by condensation is proportional to the particle cross section and to the number concentration n_c of condensable vapor molecules (Friedlander, 1977):

$$\left(\frac{dv}{dt}\right)_{cond} = an_c v^{2/3}, \tag{9}$$

where a is a constant.

Since we are assuming a size-independent coagulation rate constant, the size growth by coagulation is independent of the condensation process. This point is very important

because it implies that equation (8) is still correct even when condensation is occurring in the system. Thus, we can write

$$\frac{\mathrm{d}v}{\mathrm{d}t} = \left(\frac{\mathrm{d}v}{\mathrm{d}t}\right)_{\mathrm{coag}} + \left(\frac{\mathrm{d}v}{\mathrm{d}t}\right)_{\mathrm{cond}} = R_{\mathrm{coag}} v_0 P + R_{\mathrm{cond}} \frac{v_0^{1/3}}{n_{\mathrm{c0}}} n_{\mathrm{c}} v^{2/3}, \tag{10}$$

where

$$R_{\mathrm{cond}} \equiv a n_{\mathrm{c0}} v_0^{-1/3} \tag{11}$$

is the *condensation rate* (with dimensions of time^{-1}), and n_{c0} is the number concentration of vapor molecules at the tube inlet.

The number concentration of condensable vapor molecules, n_{c}, decreases with time as vapor condensation onto the particle surface takes place. This decrease with time can be determined from the total particle volume (mass) balance:

$$\frac{\mathrm{d}}{\mathrm{d}t}(Nv) = -\delta N v - v_{\mathrm{c}} \frac{\mathrm{d}n_{\mathrm{c}}}{\mathrm{d}t}. \tag{12}$$

In the last equation, v_{c} is the volume of a vapor molecule. Integration of (12) leads to

$$n_{\mathrm{c}} = n_{\mathrm{c0}} - \frac{N_0 v_0}{v_{\mathrm{c}}}\left(\frac{Nv}{N_0 v_0} - 1 + \delta \int_0^t \frac{Nv}{N_0 v_0}\,\mathrm{d}t\right). \tag{13}$$

Inserting (13) into (10), the time variation of the mean particle volume due to coagulation, condensation, and diffusion losses can be finally expressed as

$$\frac{\mathrm{d}v^*}{\mathrm{d}t} = R_{\mathrm{coag}} P + R_{\mathrm{cond}} (v^*)^{2/3}\left[1 - V_{\mathrm{pc}}^*\left(V_{\mathrm{T}}^* - 1 - \frac{\ln P}{t}\int_0^t V_{\mathrm{T}}^*\,\mathrm{d}t\right)\right], \tag{14a}$$

where

$$v^* = \frac{v}{v_0} \tag{14b}$$

is the relative particle mean volume increase;

$$V_{\mathrm{pc}}^* = \frac{N_0 v_0}{n_{\mathrm{c0}} v_{\mathrm{c}}} \tag{14c}$$

is the ratio of total particle volume to total condensable vapor molecule volume at the tube inlet (it is thus a measure of the degree of completion of the condensation process in the cooling section of the aerosol generator); and

$$V_{\mathrm{T}}^* = \frac{Nv}{N_0 v_0} \tag{14d}$$

is the total particle volume relative increase.

v^*, $\mathrm{d}v^*/\mathrm{d}t$ and V_{T}^* can be determined from experimental measurements. The coagulation rate R_{coag} can also be determined from experiments using equation (4) and the known value of particle penetration P at time t. Therefore, from experiments one can determine the condensation rate R_{cond} and the initial total particle-to-vapor molecule volume ratio V_{pc}^*. Indeed, according to (14), a plot of $[(\mathrm{d}v^*/\mathrm{d}t) - R_{\mathrm{coag}} P](v^*)^{-2/3}$ against $[V_{\mathrm{T}}^* - 1 - (\ln P)(\int_0^t V_{\mathrm{T}}^*\,\mathrm{d}t)/t]$ should yield a straight line of slope $(-R_{\mathrm{cond}} V_{\mathrm{pc}}^*)$ and y-intercept R_{cond}.

EXPERIMENTAL METHOD

The experimental set up is shown in Fig. 1. Clean dry air of 2 l min^{-1} is passed through a tube furnace where a small amount of NaCl is heated to 720°C. The vapor thus formed is then cooled down in a water bath whose temperature is kept at a preset value. The aerosol

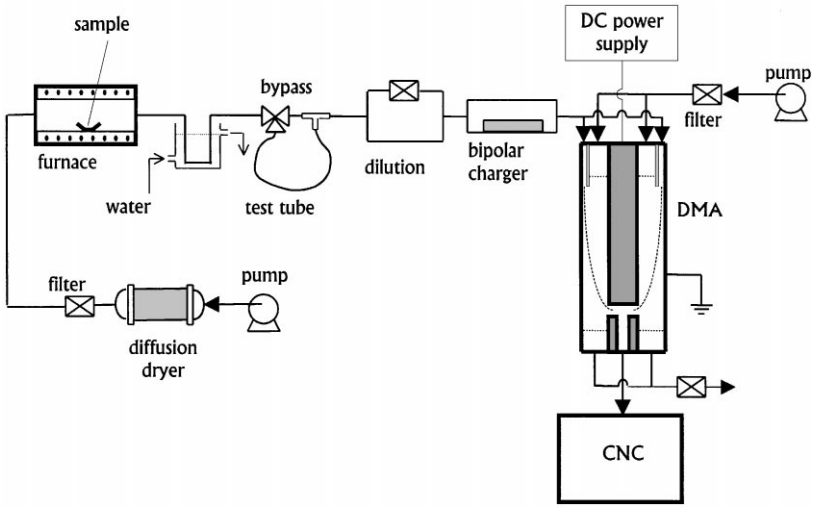

Fig. 1. Experimental set-up.

particles leaving the water bath are then alternately passed through either a test tube or a bypass route which is used as a reference. The plastic test tube between the three-way valve and the T-tube has ID 10 mm (OD 14 mm) and variable lengths to give the desired aerosol mean residence time. The bypass route consists in a very short plastic tube connecting the remaining outlet of the three-way valve and the T-tube in such a way that the valve and the T-tube are actually in contact with each other.

Just after the testing section the aerosol is diluted by passing part of it through a filter. The aim of dilution is to make sure that particles do not coagulate beyond the testing section. However, aerosol particles are presumably still growing by condensation all the way between the testing section and the particle measurement system.

The diluted aerosol is then electrically charged in a Kr-85 neutralizer (TSI 3077), and classified in a differential mobility analyzer (DMA, TSI short column). The DMA operates with aerosol flow rate of $2\,\mathrm{l\,min^{-1}}$ (inlet = sampling), and sheath air flow rate of $20\,\mathrm{l\,min^{-1}}$ (inlet = excess). Particle concentrations were measured with a condensation nucleus counter (CNC, TSI 3025).

In each experiment, the particle size distribution was measured for the aerosol passing through the bypass route, and immediately after for that passing through the test tube. For each tube length, three such runs were done. The results reported below are averages of three runs. Experiments were done with water bath temperatures of 0, 20 and 45°C (gas temperature at the outlet of the bath of 3, 22 and 45°C, respectively). The mean aerosol residence time in the cooling section (water bath) was 0.1 s.

The CNC-measured concentrations were corrected to account for charging probability (as recently measured by us, Alonso *et al*., 1997b), CNC counting efficiency (Wiedensohler *et al*., 1997), and DMA penetration (Fissan *et al*., 1998); these are by large the most important sources of particle "losses" in the system. The particle mean volume diameter and the total particle number concentration were calculated from the corrected concentrations. The measurements for the bypass route give the values of v_0 and N_0; those for the test tube give the values of v and N.

DMA sizing errors due to Brownian diffusion-induced *voltage shifts* have not been taken into account. This is permissible as long as one is only interested in mean particle diameters since, as previously demonstrated (Alonso and Kousaka, 1996; Alonso *et al*., 1998), voltage shifts are negligible around the size distribution peak.

Preliminary experiments, in which the aerosol was directly admitted into the DMA-CNC system bypassing the Kr-85 neutralizer, showed that NaCl particles leaving the generator were uncharged. Thus, electrostatic effects in the test tube were absent. The two outlets of the three-way valve were also checked and shown to give particle penetrations quite similar.

RESULTS AND DISCUSSION

Typical size distributions obtained in the course of this work are plotted in Fig. 2. The actual particle number concentrations are higher than reported because the aerosol dilution after the testing section has not been taken into account in the calculations (of course, the dilution was the same for all the experiments). As seen, we have worked with quite small particles, with initial mean volume diameter between 4 and 5 nm depending on the cooling water temperature (see Table 1), because it is in these extremely small particles where condensation growth can compete with coagulation.

Figure 3 shows the total particle volume increase with time. If condensation were finished in the generator's cooling section, i.e. if there were no condensable vapor molecules at the test tube inlet ($t = 0$), the total particle volume should decrease with time because of diffusion losses (see equation (6)). As Fig. 1 shows, the total particle volume increased in all the experiments. In spite of this experimental fact, we still can suppose that condensation occurs only in the cooling section and not in the test tube; for this to be true we must then accept that some of the incipient particles formed in the cooling section have no time to reach a size detectable by the instruments (either because the charging probability is too small or because the CNC counting efficiency drops to zero). That is, at time $t = 0$ we might have "large" (detectable) particles and "small" (undetectable) particles; in the tube ($t > 0$) the small particles coagulate among themselves and also with the large ones, resulting in a total particle volume increase ($Nv/N_0v_0 > 1$). However, if this explanation were correct, the number concentration of small and large particles at time $t = 0$ should both decrease as the water bath temperature increases; hence, for higher cooling temperature we should expect smaller total particle volume increase in the test tube. But the trend shown by the experimental data in Fig. 3 is just the reverse.

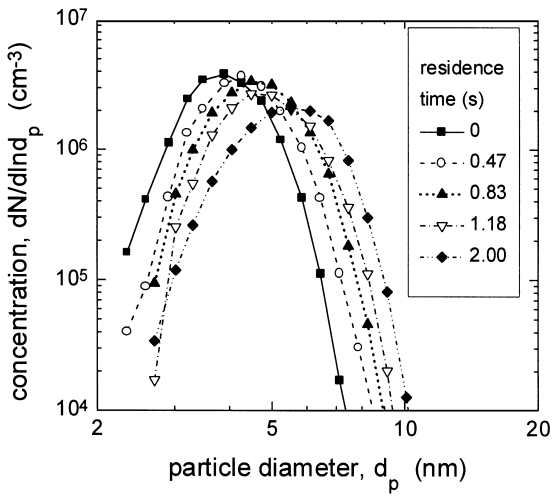

Fig. 2. Typical time-evolution of the particle size distribution. Water bath temperature: 45°C.

Table 1. Coagulation and condensation rates as a function of the cooling water temperature. T = cooling water temperature; D_{v0} = mean volume diameter at time $t = 0$ (test tube inlet); R_{coag} = coagulation rate; R_{cond} = condensation rate; $V^*_{pc} = N_0v_0/n_{c0}v_c$ = initial total particle volume to condensable vapor molecule volume ratio

T (°C)	D_{v0} (nm)	R_{coag} (s^{-1})	R_{cond} (s^{-1})	V^*_{pc} (−)	R_{cond}/R_{coag} (−)
0	5.00	0.15	0.66	0.43	4.40
20	4.51	0.11	0.70	0.38	6.36
45	3.99	0.09	0.71	0.34	7.89

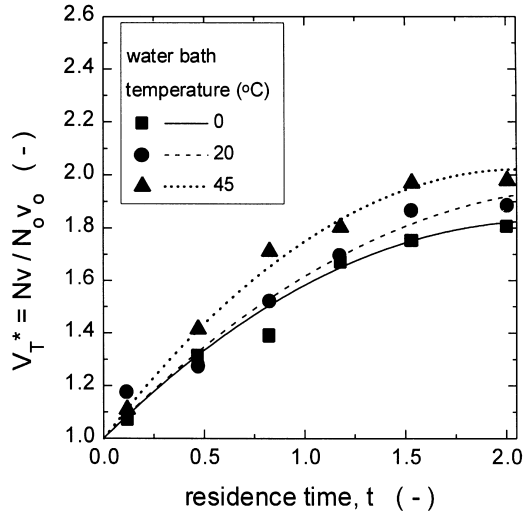

Fig. 3. Total particle volume increase in the test tube as a function of the cooling water temperature. Symbols are experimental data. Lines are 2nd order polynomial fittings of the form $V_T^* = 1 + c't + ct^2$.

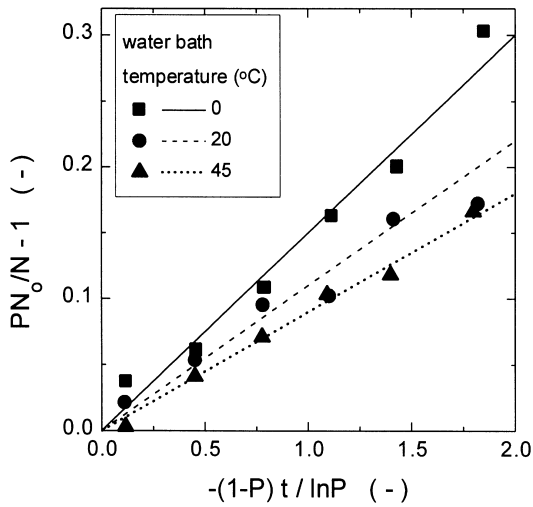

Fig. 4. Evaluation of the coagulation rate R_{coag} from experimental data (symbols). Lines are least square fittings whose slopes give the values of R_{coag}.

Therefore, it must be concluded that condensation *does* indeed take place in the test tube. Furthermore, the trend of the curves in Fig. 3 agrees qualitatively with the reasonable expectation that higher cooling temperature implies larger amount of condensable vapor at $t = 0$ and, hence, larger total particle volume increase by condensation in the tube.

The coagulation rate can be determined from the experimental data by plotting $[(PN_0/N) - 1]$ against $[-(1 - P)t/\ln P]$. This plot is presented in Fig. 4 for different cooling water temperatures. According to equation (4), the slope of these lines gives the coagulation rate R_{coag}. Although penetration has been included in the model in the simple form $P = e^{-\delta t}$, the values of P used in Fig. 4 (and in the rest of the figures) have been calculated using the rigorous equation of Gormley and Kennedy, equation (1), evaluated for the particle mean volume diameter at time $t = 0$ (D_{v0} in Table 1). Table 1 shows the coagulation rates as a function of the cooling water temperature. Intuitively, one expects that lower cooling temperature results in higher particle number concentration and larger mean particle size at time $t = 0$; thus, the coagulation rate should increase with decreasing cooling water temperature, in agreement with the experimental results.

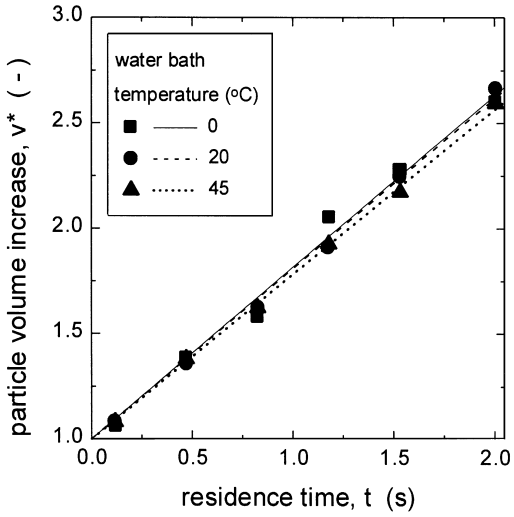

Fig. 5. Particle mean volume increase $v^* = v/v_0$ as a function of cooling water temperature. Symbols are experimental data. Lines are fittings of the form $v^* = 1 + ct$.

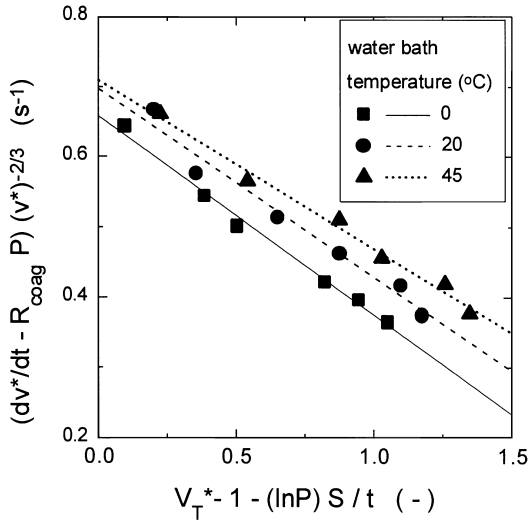

Fig. 6. Determination of the condensation rate R_{cond} from experimental data. In the x-axis legend, $S = \int_0^t V_T^* \, dt$. The slopes of the least-square fitting lines give the values of $R_{\text{cond}} V_{pc}^*$; the y-intercepts give the values of R_{cond}.

Once the coagulation rate is known, we can use equation (14) to determine the condensation rate R_{cond}. For this one must evaluate dv^*/dt and $\int_0^t V_T^* \, dt$. We have proceeded as follows. The experimental data of mean particle volume increase was fitted by linear expressions of the form $v^* = 1 + ct$, where c is a constant. The fittings, shown in Fig. 5, led to $c = 0.82$, 0.81 and 0.78 s^{-1} for cooling temperatures of 0, 20 and 45°C, respectively. Note that the derivative dv^*/dt is simply given by the constant c. The total particle volume increase $V_T^* = Nv/N_0 v_0$ was fitted by second-order polynomials, $V_T^* = 1 + c't + c''t^2$; the fittings, shown in Fig. 3, led to $c' = 0.75$, 0.77 and 0.99 s^{-1}, and $c'' = -0.17$, -0.16 and -0.24 s^{-2}, for water bath temperatures of 0, 20 and 45°C, respectively. The integral $\int_0^t V_T^* \, dt$ was calculated using the fitting polynomials. According to equation (14), the y-intercepts of the lines plotted in Fig. 6 give directly the condensation rates R_{cond}. The slopes give the values of $R_{\text{cond}} V_{pc}^*$. The numerical values thus obtained are listed in Table 1. The trend of the results is also reasonable. The condensation rate increases (not appreciably, however) with the cooling water temperature because, as already pointed out, higher

cooling water temperature implies large amount of condensable vapor in the tube. This is more clearly seen in the fifth column of Table 1, which corresponds to the ratio of total particle volume to total condensable molecule volume at time $t = 0$; this ratio clearly decreases with the cooling water temperature for a double reason: less particles are formed and more vapor remains uncondensed. The last column in Table 1 shows the relative importance of condensation and coagulation in the tube; the numerical results in this case are markedly different among each other and the trend is, again, in perfect agreement with the expectations.

However, the interpretation of these results should be done with care because condensation growth is likely to be occurring far beyond the testing section. If this is true, the actual condensation rate in the test tube is actually smaller than the values we have reported here. The calculated coagulation rates are more reliable because (a) the aerosol dilution device practically prevents coagulation to occur beyond the test section, and (b) R_{coag} is calculated from the measured concentrations N and N_0, which are not affected by condensation (if one assumes that particle formation by homogeneous nucleation in the tube is comparatively negligible!)

CONCLUSIONS

A model has been presented which can be used to evaluate the relative importance of coagulation and condensation in systems where aerosol particles simultaneously grow by both mechanisms. Diffusion losses have been incorporated into the model in an approximate manner. It has been shown that aerosol particles generated by a conventional evaporation–condensation technique still grow by condensation downstream far beyond the generator. This point is very important, and it should be always kept in mind whenever one uses evaporation–condensation aerosols to test theories of phenomena (coagulation, filtration, charging) taking for granted that further condensational growth is absent. This problem is particularly important in the case of nanometer-sized aerosols, where the size growth by condensation can be of the same order of magnitude as the coagulation growth.

Acknowledgments—This work was partly supported by the Spanish Ministerio de Educación y Cultura, DGES, Grant PB96-0920. We also wish to express our gratitude to the Referees of this paper for their positive critics and suggestions.

REFERENCES

Alonso, M. and Kousaka, Y. (1996) *J. Aerosol Sci.* **27,** 1201.
Alonso, M., Kousaka, Y., Hashimoto, T. and Hashimoto, N. (1997a) *Aerosol Sci. Tecnol.* **27,** 471.
Alonso, M., Kousaka, Y., Nomura, T., Hashimoto, N. and Hashimoto, T. (1997b) *J. Aerosol Sci.* **28,** 1479.
Alonso, M., Kousaka, Y., Hashimoto, T. and Hashimoto, N. (1998) *J. Aerosol Sci.* **29,** 985.
Davies, E. J. and Liao, S. C. (1975) *J. Colloid Interface Sci.* **50,** 488.
Friedlander, S. K. (1977) *Smoke, Dust and Haze.* Wiley, New York.
Fissan, H., Pöcher, A., Neumann, S., Boulaud, D. and Pourprix, M. (1998) *J. Aerosol Sci.* **29,** 289.
Gormley, P. G. and Kennedy, M. (1949) *Proc. Roy. Irish Acad.* **52,** 163.
Jain, S., Kodas, T. T., Wu, M. K. and Preston, P. (1997) *J. Aerosol Sci.* **28,** 133.
Katoshevski, D. and Seinfeld, J. H. (1997) *Aerosol Sci. Technol.* **27,** 550.
Lazaridis, M. and Koutrakis, P. (1997) *J. Aerosol Sci.* **28,** 107.
Pesthy, A. J., Flagan, R. C. and Seinfeld, J. H. (1983) *J. Colloid Interface Sci.* **91,** 525.
Phanse, G. M. and Pratsinis, S. E. (1989) *Aerosol Sci. Technol.* **11,** 100.
Pratsinis, S. E. (1988) *J. Colloid Interface Sci.* **124,** 416.
Seigneur, C., Hudischewskyi, A. B., Seinfeld, J. H., Whitby, K. T., Whitby, E. R., Brock, J. R. and Barnes, H. M. (1986) *Aerosol Sci. Technol.* **5,** 205.
Warren, D. R. and Seinfeld, J. H. (1985) *Aerosol Sci. Technol.* **4,** 31.
Wiedensohler, A., Orsini, D., Covert, D. S., Coffmann, D., Cantrell, W., Havlicek, M., Brechtel, F. J., Russell, L. M., Weber, R. J., Gras, J., Hudson, J. G. and Litchy, M. (1997) *Aerosol Sci. Technol.* **27,** 224.
Wilck, M. and Stratmann, F. (1997) *J. Aerosol Sci.* **28,** 959.
Wu, C. Y. and Biswas, P. (1998) *Aerosol Sci. Technol.* **28,** 1.
Zhang, Z. Q. and Liu, B. Y. (1990) *Aerosol Sci. Technol.* **13,** 493.